

Journal of Experimental Botany https://doi.org/10.1093/jxb/erab393 Advance Access Publication 9 September, 2021



#### RESEARCH PAPER

# Cadmium interference with iron sensing reveals transcriptional programs sensitive and insensitive to reactive oxygen species

Samuel A. McInturf<sup>1,\*</sup>, Mather A. Khan<sup>1,\*,</sup>, Arun Gokul<sup>2</sup>, Norma A. Castro-Guerrero<sup>1,</sup>, Ricarda Höhner<sup>3</sup>, Jiamei Li<sup>5</sup>, Henri-Baptiste Marjault<sup>6</sup>, Yosef Fichman<sup>1</sup>, Hans-Henning Kunz<sup>3,4,</sup>, Fiona L. Goggin<sup>5</sup>, Marshall Keyster<sup>2</sup>, Rachel Nechushtai<sup>6</sup>, Ron Mittler<sup>1</sup> and David G. Mendoza-Cózatl<sup>1,2,†,</sup>

- <sup>1</sup> Division of Plant Sciences, C.S. Bond Life Sciences Center, University of Missouri, Columbia, MO 65211, USA
- <sup>2</sup> Environmental Biotechnology Laboratory, Department of Biotechnology, University of the Western Cape, Bellville, Cape Town, 7535, South Africa
- <sup>3</sup> School of Biological Sciences, Washington State University, PO Box 644236, Pullman, WA 99164-4236, USA
- <sup>4</sup> Biozentrum der LMU München, Germany
- <sup>5</sup> Department of Entomology and Plant Pathology, 217 Plant Sciences Building, University of Arkansas System Division of Agriculture, Fayetteville, AR 72701, USA
- <sup>6</sup> Institute of Life Science, The Hebrew University of Jerusalem, Jerusalem, 91904 Israel
- \* These authors contributed equally to this work.
- <sup>†</sup> Correspondence: mendozad@missouri.edu

Received 20 May 2021; Editorial decision 13 August 2021; Accepted 25 August 2021

Editor: Ann Cuypers, Hasselt University, Belgium

#### **Abstract**

Iron (Fe) is an essential micronutrient whose uptake is tightly regulated to prevent either deficiency or toxicity. Cadmium (Cd) is a non-essential element that induces both Fe deficiency and toxicity; however, the mechanisms behind these Fe/Cd-induced responses are still elusive. Here we explored Cd- and Fe-associated responses in wild-type Arabidopsis and in a mutant that overaccumulates Fe (opt3-2). Gene expression profiling revealed a large overlap between transcripts induced by Fe deficiency and Cd exposure. Interestingly, the use of opt3-2 allowed us to identify additional gene clusters originally induced by Cd in the wild type but repressed in the opt3-2 background. Based on the high levels of H<sub>2</sub>O<sub>2</sub> found in opt3-2, we propose a model where reactive oxygen species prevent the induction of genes that are induced in the wild type by either Fe deficiency or Cd. Interestingly, a defined cluster of Fe-responsive genes was found to be insensitive to this negative feedback, suggesting that their induction by Cd is more likely to be the result of an impaired Fe sensing. Overall, our data suggest that Fe deficiency responses are governed by multiple inputs and that a hierarchical regulation of Fe homeostasis prevents the induction of specific networks when Fe and H<sub>2</sub>O<sub>2</sub> levels are elevated.

Keywords: Cadmium toxicity, iron sensing, leaf ferrome, long-distance signaling, reactive oxygen species.

# Page 2 of 15 | McInturf et al.

# Introduction

Iron (Fe) is an essential nutrient for all known biological systems, facilitating the transfer of electrons and acting as a cofactor in metalloproteins. While vital for life, Fe is also extremely reactive, producing free radicals when Fe is in excess. For this reason, Fe uptake, storage, and allocation have to be properly sensed and tightly regulated to prevent either deficiency or toxicity (Khan *et al.*, 2014).

Fe is abundant in most soils, although it is typically found as insoluble Fe<sup>3+</sup> complexes and therefore unavailable for uptake into root cells (Römheld and Marschner, 1986). In turn, land plants have evolved two strategies to overcome the challenge of solubilizing and importing Fe into roots from the rhizosphere. Strategy I is a reduction strategy carried out at the plasma membrane where membrane-bound reductases directly reduce Fe<sup>3+</sup> to Fe<sup>2+</sup> prior to transport across the membrane by transporters of the ZIP family (reviewed by Hindt and Guerinot, 2012). Strategy II is a chelation strategy, which is mediated by the release of phytosiderophores such as deoxymugineic acid (DMA) into the rhizosphere, where a soluble Fe<sup>3+</sup>–DMA complex is formed and imported into roots by transporters of the *Yellow Stripe* family (Curie *et al.*, 2001, 2009; Inoue *et al.*, 2009; Lee *et al.*, 2009).

Dicots, such as Arabidopsis, utilize Strategy I and form the core of our understanding of Fe uptake and its regulation during changes in Fe availability. In these plants, Fe<sup>3+</sup> is initially released from negatively charged soil particles by acidification of the rhizosphere through the P-type ATPase AHA2 (Santi and Schmidt, 2009). Once released from the soil particles, Fe<sup>3+</sup> is reduced to Fe<sup>2+</sup> by the transmembrane protein ferric reduction oxidase 2 (FRO2) (Robinson *et al.*, 1999). Finally, Fe<sup>2+</sup> is transported into the root primarily by iron regulated transporter 1 (IRT1). While IRT1 has high affinity towards Fe<sup>2+</sup>, it is also able to transport a broad range of divalent metals including zinc, manganese, and the non-essential element cadmium (Cd) (Korshunova *et al.*, 1999).

Transcriptional regulation of the Fe uptake machinery is primarily mediated by the FIT network, which consists of five basic helix-loop-helix (bHLH) transcription factors (TFs) of the subgroup Ib: FIT (bHLH029), bHLH38, bHLH39, bHLH100, and bHLH101 (Yuan et al., 2008; Sivitz et al., 2012; Wang et al., 2013). These genes are under independent regulatory schemes but they are thought to function as homo- and heterodimers, allowing for multiple input signals to induce or repress Fe uptake. During prolonged Fe deficiency or H<sub>2</sub>O<sub>2</sub> exposure, the zinc finger transcription factor ZAT12 is induced and represses FIT activity, thereby inhibiting Fe uptake and preventing further Fe excess-mediated oxidative damage (Le et al., 2016). Additionally, Fe uptake is regulated by the plant hormones ethylene, cytokinins, jasmonates, auxin, and the signaling molecule nitric oxide (Hindt and Guerinot, 2012). FIT has been shown to interact with additional TFs such as EIN1 and EIL3 to promote Fe uptake by stabilizing FIT (Lingam et al., 2011; Yang et al., 2014) while the presence of nitric oxide prevents the 26S proteasome-mediated degradation of FIT (García et al., 2010).

While the transcriptional regulation of IRT1 and associated genes involved in root Fe uptake is mediated by the FIT network, a second clade of bHLH proteins, the PYE network, regulates intracellular Fe homeostasis. The founding member of this clade, POPEYE (PYE), was found to be induced by Fe deficiency in roots (Long et al., 2010). In addition to PYE itself, the PYE network is composed of PYE-like proteins (PYEL) bHLH34, bHLH104, bHLH115, and ILR3 (Zhang et al., 2015; Li et al., 2016; Liang et al., 2017), as well as BRUTUS (BTS), an E3 ubiquitin ligase that degrades PYEL proteins to prevent Fe overaccumulation (Long et al., 2010; Selote et al., 2015; Hindt et al., 2017). The PYE network, like the FIT network, is thought to operate by hetero- and homodimerization of TFs, which then bind to the promoters of key Fe homeostasis genes such as ZIF1, NAS4, and FRO3 (Long et al., 2010), as well as bHLH38/39/100/101 (Zhang et al., 2010; Li et al., 2016; Liang et al., 2017).

Though the components of the Fe uptake machinery in roots have been known for years, the mechanisms behind Fe sensing and signaling at the whole-plant level is an ongoing active area of research. Arabidopsis is known to have at least two distinct Fe-sensing systems, a local sensing system in roots, and a systemic sensing system in leaves (Khan *et al.*, 2018). The systemic sensing system allows the leaves to dictate the amount of Fe to be acquired by roots, while the local sensing system allows individual roots to regulate their response to their local environment, mostly through post-translational mechanisms (Barberon *et al.*, 2011; Sivitz *et al.*, 2011; Guillaume *et al.*, 2018).

Cadmium, on the other hand, is a non-essential element that shares chemical properties with Fe and therefore is capable of entering root cells using the Fe uptake system (Meda et al., 2007; Wu et al., 2012; Lešková et al., 2017). Cd has been shown to induce genes such as IRT1 and OPT3, which are usually induced under Fe-limiting conditions; however, whether this Fe deficiency-like response is only due to direct competition and reduced Fe uptake in the presence of Cd, or whether Cd directly impairs the Fe-sensing mechanism is currently not known. Notably, co-expression of FIT and AtbHLH38/39 enhanced Cd tolerance in Arabidopsis by promoting increased Cd sequestration in roots (Wu et al., 2012). More recently, there have been significant advances in defining Fe-responsive gene networks in a tissue- and cellspecific manner (Khan et al., 2018). In this work, we used low levels of Cd to probe whether this non-essential element directly impairs Fe sensing in wild-type plants and in a mutant that overaccumulates Fe in leaves and roots (opt3-2). Our results show that Cd does induce a transcriptional program consistent with Fe deficiency in wild-type leaves and roots. However, many of these genes were not induced by Cd in opt3-2. Notably, despite the presence of high levels of Fe in opt3 leaves, Cd consistently induced a specific core of Fe-responsive genes known to be localized in the leaf vasculature. Further analyses demonstrate that genes originally induced by Cd in wild-type plants, but not in opt3-2 (Fe excess conditions), belong to networks associated with pathogen responses and oxidative stress. Taken together, our results suggest that when plants experience opposite cues (Fe deficiency and high  $H_2O_2$ ), there is a hierarchical regulation of Fe homeostasis in which  $H_2O_2$  over-rides the induction of a subset of genes that otherwise would have been induced by Fe deficiency.

# Materials and methods

#### Plant growth and luciferase imaging

Arabidopsis wild-type (Col-0) and *opt3-2* plants were germinated on 1/4 Murashige and Skoog (MS) agar plates after 2 d of stratification at 4 °C in the dark. After ~10 d, plants were transferred to replete hydroponic media as previously described (Khan *et al.*, 2018). The solution was changed every 2 d and aerated with small aquarium-type air pumps. At bolting, fresh solution with the indicated concentrations of CdCl<sub>2</sub> was added for 72 h. The *opt3-2*×OPT3p::Luc line was generated by crossing the Col-0 carrying the OPT3p::Luc insertion reported in Khan *et al.* (2018) with *opt3-2*. Homozygous *opt3-2*×OPT3p::Luc plants (F<sub>2</sub>) were identified by PCR (for the *opt3-2* insertion described in Mendoza-Cozatl *et al.*, 2014) and 100% luminescence in the corresponding F<sub>3</sub> progeny. Luminescence and the corresponding paired bright field images were acquired using a UVP BioImaging Systems EpiChemi3 Darkroom system (15 min exposure time, 4×4 binning settings).

# RNA sequencing and data analysis

Leaves and roots were harvested separately and pulverized in a mortar and pestle cooled with liquid nitrogen. mRNA was purified using a EZ Plant RNA kit (Qiagen, Germany) and contaminant DNA was removed using a TURBO DNase kit (Invitrogen, USA). Total RNA was submitted to the University of Missouri Core Facility for 100 bp Illumina sequencing. The resulting reads were trimmed such that all bases were called at a 95% accuracy using ShortRead (Morgan et al., 2009) and mapped to the TAIR 10 genome release using TopHat (Kim et al., 2013). The remaining analysis was carried out in R and Bioconductor (Huber et al., 2015; R Core Team, 2018). Feature counting was performed using ShortRead (Morgan et al., 2009), and 92% of raw reads were uniquely mapped. Differential expression was called using edgeR (Robinson et al., 2010), and heatmaps and Venn diagrams were generated in gplots (Warnes et al., 2016). Ontology enrichment tests were performed using GOstats (Falcon and Gentleman, 2007) utilizing the conditional hypergeometric test with a P-value cut-off of 0.05. The union of the Fe excess-dependent and Fe excess-independent values was used as the gene universe for each test, for leaves and roots independently. Previously published sequencing data (without Cd treatment) can be found on NCBI GEO GSE79275, while those of the Cd-exposed sample can be found as GSE128156. These datasets comprise the SuperSeries GSE128157.

#### Assembly of the expanded root ferrome and leaf ferrome

The expanded root ferrome and leaf ferrome (Supplementary Table S1) were assembled using tissue-specific Fe deficiency microarray profiling experiments from Stein and Waters (2012) (ecotypes Kas and Tsu after 24 h and 48 h Fe deficiency) and Kumar *et al.* (2017) (ecotype Col-0 after 72 h Fe deficiency). Each dataset was analyzed using GEO2R (Barrett

et al., 2013), and fold changes associated with Benjamini and Hochberg-moderated P-values > 0.05 were set to zero (Benjamini and Hochberg, 1995). For the Kumar dataset, the expected direction of regulation was determined by the sign (positive or negative) of the log<sub>2</sub> fold change. For the Stein dataset, an expected direction of regulation was determined for each ecotype by taking the sign of the latest non-zero fold change. A consensus direction of regulation was determined by first constructing an array of fold change signs for each ecotype and sorted under the following rules: genes with two zero fold changes are declared no change, one zero fold change and two similarly signed fold changes are declared up or down according to the similar fold changes, and genes with no zero fold changes are declared up or down according to the most prevalent sign. The previously published ferrome was appended to genes identified in roots. The direction of regulation of ferrome genes not identified here was inferred from Buckhout et al. (2009).

#### Hydrogen peroxide quantification

H<sub>2</sub>O<sub>2</sub> concentrations in leaves were determined by the method described in Velikova *et al.* (2000). Briefly, 500 mg of fresh tissue was homogenized on ice in a solution of 0.1% trichloroacetic acid and the debris was pelleted at 12 000 g. A 0.5 ml aliquot of the supernatant was added to 0.5 ml of 10 mM potassium phosphate buffer (pH 7) and 1 ml of 1 M KI. The absorbance at 390 nm was read and compared with a standard curve of H<sub>2</sub>O<sub>2</sub>. In roots, H<sub>2</sub>O<sub>2</sub> was quantified using the Amplex Red reagent (Thermo Fisher Scientific, USA), according to the methods of Brumbarova *et al.* (2016). Oxidation of Amplex Red to resorufin was measured by quantifying resorufin fluorescence with excitation at 545 nm and emission at 590 nm. Statistical differences between genotypes and treatments were calculated using the two-sample *t*-tests script in R.

#### Dynamic H<sub>2</sub>O<sub>2</sub> imaging

Plants were fumigated with 100 µM of the H<sub>2</sub>O<sub>2</sub> oxidation-activated dye Peroxy Orange 1 (PO1; Millipore-Sigma, St. Louis, MO, USA) in 50 mM phosphate buffer (pH 7.4) with 0.01% (v/v) Silwet L-77 (PlantMedia-Bio-World, Dublin, OH, USA) for 30 min, using a portable nebulizer (Punasi Direct, Hong Kong, China), as described in Fichman et al. (2019). For oxidation inhibition treatment, prior to the dye fumigation, plants were fumigated with 10 mM ascorbic acid (Millipore-Sigma) for 30 min. Fluorescence images (excitation/emission 540 nm/620 nm) were acquired with an IVIS Lumina S5 apparatus (PerkinElmer, Waltham, MA, USA) with a defined optic setting of FOV: 15, f2, 5 s exposure. Images were analyzed using Living Image 4.7.2 software (PerkinElmer), as described in Fichman et al. (2019). Total radiant efficiency was used for calculations. Time-lapse images of H2O2 accumulation in oxidation inhibition experiments were obtained by using the math tools option in the software. Statistical analysis was performed using Microsoft Excel with SE, followed by Student's t-test (Fichman et al., 2019). Glutathione and DTT (10 mM) infiltration were conducted in detached shoots submerged in the corresponding solution for 10 min before plants were sprayed with 5 mM luciferin dissolved in sterile water containing 0.1% Triton X-100 (Khan et al., 2018).

#### Photosynthetic activity

Col-0 and *opt3-2* were stratified at 4 °C in the dark and subsequently germinated on 1/4 MS media plates under long-day conditions (16 h light/8 h dark). After 14 d of growth, seedlings were transferred either to fresh 1/4 MS plates (mock control) or to 1/4 MS plates supplemented with 20  $\mu$ M Cd. Subsequently, we started to monitor plant photosynthetic performance on a daily basis by determining maximum quantum yield of PSII ( $F_{\rm v}/F_{\rm m}$ ) using a Walz Imaging PAM (Kunz *et al.*, 2009).

# Page 4 of 15 | McInturf et al.

Purification and spectroscopy of AtNEET

AtNEET stability assays were conducted at room temperature (pH 8.0) and the indicated Cd concentrations with 100 µM of purified AtNEET as previously described (Nechushtai et al., 2012). Briefly, AtNEET protein was expressed in *Escherichia coli* BL21 competent cells. At an  $\mathrm{OD}_{600\;\mathrm{nm}}$ of 0.6, FeCl<sub>3</sub> at 750 µM was added to the cell culture and incubated for an additional 16 h at 23 °C. AtNEET was purified from lysed cells using an Ni-NTA column and utilized for 2Fe-2S cluster transfer to apoferredoxin (aFed) as described by Nechushtai et al. (2012). The stability of the 2Fe-2S cluster in NEET and its ability to donate the cluster to aFed in the presence of Cd was assessed by monitoring the UV-Vis absorption spectra or the visible chromophore change in proteins separated by native-PAGE. Absorption spectra were recorded at 400-650 nm (CARY, 300Bio; Varian) with special attention given to changes in 458 nm absorbance (At-NEET signature [2Fe-2S] absorbance peak) vis-à-vis the 423 nm peak characteristic of the [2Fe-2S] cluster in Fd. A successful transfer of the [2Fe-2S] cluster between AtNEET and aFd can be traced as a reduction in the 458 nm absorption peak, characteristic of AtNEET, with a concomitant appearance of a 423 nm peak (characteristic of holo-Fd). For native-PAGE assays, AtNEET (1 mg ml<sup>-1</sup>) was incubated with aFd (1 mg ml<sup>-1</sup>) and different Cd concentrations and in the presence of 2% mercaptoethanol, 5 mM Na-dithionite, and 5 mM EDTA for the specified lengths of time. Proteins were then separated using 15% acrylamide gels.

# **Results**

Cadmium induces a transcriptional iron deficiency-like response in roots and leaves

In this work, we took advantage of the shared chemical properties of Fe and Cd, and use Cd as a chemical probe to assess Fe deficiency responses. Since plant responses to Cd vary depending on its concentration, we began this work by identifying a Cd concentration where the visual damage to leaves (i.e. chlorosis) was minimal. We included in these experiments the Arabidopsis mutant opt3-2, which constitutively overaccumulates Fe in leaves even in the presence of Cd (Mendoza-Cózatl et al., 2014; Zhai et al., 2014), thus offering a suitable background to explore Cd-induced Fe deficiency-like responses in the presence of high levels of Fe. Wild-type and opt3-2 plants were grown in replete hydroponic solution to bolting stage (~4 weeks) and then exposed to several concentrations of CdCl<sub>2</sub> for 72 h (Fig. 1). While high concentrations of Cd (>50 µM) induced leaf yellowing and necrotic lesions, exposure to up to 20 µM CdCl<sub>2</sub> for 72 h had minimal impact on plant morphology in both genotypes, the wild type and opt3-2. Therefore, we selected 20 µM CdCl<sub>2</sub> for further experiments.

To begin dissecting the wild-type and *opt3-2* responses to Cd exposure, we conducted whole-genome transcriptome analyses of leaves and roots separately. Three biological replicates of each tissue/genotype were used for Illumina sequencing and, after removal of low confidence base pairs and short reads, 716 million reads were used for calling differential expression under the overdispersed binomial model implemented in edgeR (Robinson *et al.*, 2010). To minimize unreliable fold

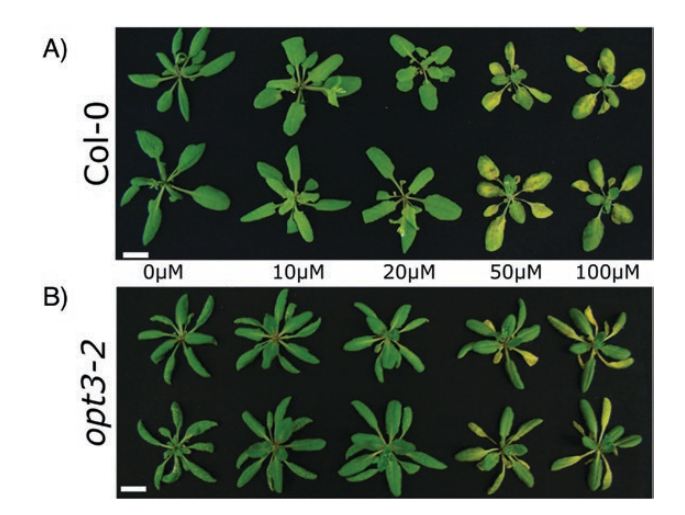


**Fig. 1.** Visual phenotypes of wild-type and <code>opt3-2</code> Arabidopsis plants exposed to cadmium for 72 h. (A) Col-0 (wild-type) and (B) <code>opt3-2</code> plants were grown in replete media for 4 weeks before being exposed to different Cd concentrations for 72 h. Cd at 20  $\mu$ M was the highest Cd concentration at which visual toxicity symptoms were minimal in both genotypes.

changes, only genes with at least 50 reads in at least one condition and absolute log₂ fold changes ≥0.5 were considered for statistical analyses (Supplementary Table S2). In wild-type plants, Cd induced changes in 3292 genes in leaves (46% induced) and 4256 genes in roots (49% induced) (Supplementary Fig. S1). A similar number of genes (3735; 46% induced) were differentially expressed in *opt3-2* leaves; however, Cd induced a substantial deregulation of transcripts in *opt3-2* roots, totaling 6527 differentially expressed genes, of which 42% were induced (Supplementary Fig. S1). Gene expression profiles and comparisons between genotypes can be visualized in absolute (FPKM) or relative (log₂ fold changes) mode through a standalone version of an electronic Fluorescent Pictograph Browser available at http://artemis.cyverse.org/david\_lab\_efp/cgi-bin/efpWeb.cgi

To determine the extent of the Fe deficiency response induced by Cd, we compared the identity of Cd-deregulated genes against datasets specific to leaves and roots containing genes deregulated (i.e. induced or repressed) under true Fe deficiency conditions. These datasets include an extended version of the published ferrome for roots (Schmidt and Buckhout, 2011) and a leaf-specific dataset that contains genes consistently affected by Fe availability across several transcriptome datasets where leaves were analyzed separately from roots (Stein and Waters, 2012; Kumar et al., 2017). In total, the leaf dataset (leaf ferrome, Supplementary Table S1) included 239 genes (172 induced, 67 repressed) while the root dataset (Supplementary Table S1) contains 406 genes (250 induced, 156 repressed). By using these datasets, we were able to assess the degree of Fe deficiency response elicited by Cd. For instance, in wildtype leaves, we found a significant overlap between Fe deficiency responses and Cd exposure, with 82 genes induced and 41 repressed. These numbers represent 48% (induced genes) and 61% (repressed genes) of the true Fe deficiency response from the leaf ferrome (Fig. 2A). Examples of genes deregulated by Cd and Fe in leaves include *IMA3* (up-pregulated ~5 log<sub>2</sub> fold), which encodes a short polypeptide known to be involved in Fe deficiency responses (Grillet *et al.*, 2018; Hirayama *et al.*, 2018), jasmonic acid signaling marker *PDF1.2* (induced ~9 log<sub>2</sub> fold) (Ahmad *et al.*, 2011; Zarei *et al.*, 2011; Cabot *et al.*, 2013), and *FER4* (repressed ~2 log<sub>2</sub> fold), which encodes a

ferritin isoform. Not all Fe deficiency-related transcripts were found to be deregulated by Cd exposure. For example, neither *CGLD27* (Urzica *et al.*, 2012) nor a key regulator of salicylic acid response *SARD1* was induced (Wang *et al.*, 2011). Similar trends were found in roots: 118 genes were induced and 60 repressed, which represents 47% of induced and 38% of repressed genes present in the expanded root ferrome (Fig. 2B). These results suggest that Cd induces a partial but significant Fe deficiency-like response in both leaves and roots.

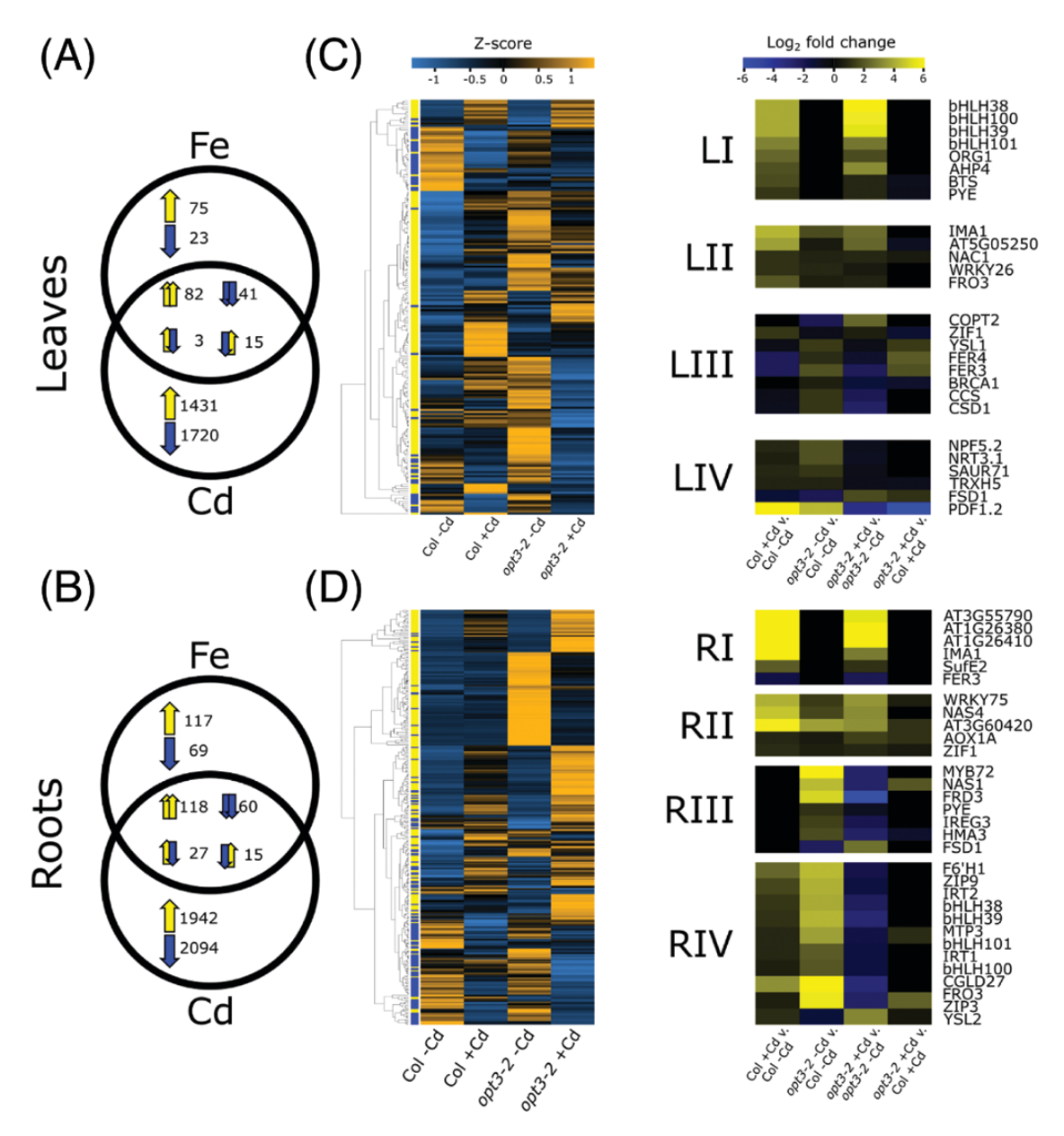


**Fig. 2.** Cadmium induces an iron deficiency response in leaves and roots. (A and B) Of all of the genes that are consistently responsive to Fe limitation in wild-type Arabidopsis plants, approximately half of them are also responsive to Cd in leaves (A) and roots (B). The pair of arrows in each intersection indicate induction/repression for Cd exposure (left arrow within each pair) and Fe deficiency (right arrow within each pair). (C and D) Genes deregulated by Fe deficiency and Cd exposure in wild-type plants and *opt3-2* were hierarchically clustered according to their log<sub>2</sub> fold changes and colored according to their gene-wise *Z*-scores for leaves (C) and roots (D), left panels. Clusters with specific trends were grouped into four groups for leaves and roots (right panels, LI–RV) and shown as log<sub>2</sub> fold changes between genotypes and treatments.

# Page 6 of 15 | McInturf et al.

Iron overload partially restricts the Cadmium-induced iron deficiency response

Cd-induced Fe deficiency responses are often attributed to the competition of Fe and Cd for the same root uptake system (i.e. IRT1, Connolly *et al.*, 2002; Lešková *et al.*, 2017). Therefore, we decided to explore if Cd was still able to induce an Fe deficiency-like response in tissues with high levels of Fe. The Arabidopsis mutant *opt3-2* has been shown to overaccumulate Fe in leaves and roots in the presence of Cd (Mendoza-Cózatl *et al.*, 2014). Moreover, the *opt3-2* leaf transcriptome is consistent with adequate sensing of Fe excess, while roots display a constitutive Fe deficiency response despite accumulating high levels of Fe (Khan *et al.*, 2018). For this analysis, we employed hierarchical clustering of all genes differentially expressed in at least one comparison between the four treatment groups: wild-type and *opt3-2* plants exposed or not to 20 µM CdCl<sub>2</sub> (Fig. 2C, D).

To streamline the simultaneous inspection across all genotypes and treatments, the clustering scheme is presented as the mean of counts per million (CPM). Using this approach, we were able to identify several distinct patterns for leaves (LI-LIV) and roots (RI-RIV) (Fig. 2C, D; Supplementary Table S2). Briefly, group I (either LI or RI) consists of genes which are similarly affected by Cd in both the wild type and opt3-2. Genes in group II are deregulated in opt3-2 relative to Col-0 prior to Cd treatment but they are similarly induced after Cd exposure. Group III comprises genes which were initially deregulated in opt3-2 relative to the wild type in the absence of Cd but, interestingly, Cd exposure reversed the sign of these genes in opt3-2. Finally, genes in group IV have a similar pattern as group III, but the magnitude of the changes was substantially different. Specific examples of genes within these clusters can be further separated in a tissue-specific manner. For instance, group LI in leaves contains vascular localized genes such as bHLH38, bHLH39, bHLH100, and bHLH101 as well as PYE, BTS, and ORG1. All these genes were induced by Cd independently of the background genotype (Fig. 2C). FRO3, however, is induced by Cd exposure in the wild type and opt3-2, but it was already induced in opt3-2 prior to Cd exposure; hence its placement in group LII. Group LIII represents a very interesting group of genes including CSD1 and its chaperone CCS, YSL1, FER3/4, and ZIF1. These genes were induced in opt3-2 but, when Cd stress was imposed, they switched from induction to repression. Group LIV contains genes such as PDF1.2, an ethylene- and jasmonate-responsive plant defensin which is highly induced by Cd stress, induced in the opt3-2 background, but repressed once opt3-2 is treated with Cd.

The transcriptional program elicited by Cd in roots was far more complex than the leaf patterns in both genotypes. For instance, gene group RI did not contain the Ib bHLHs as found in LI (Fig. 2C, D); instead, the transmembrane protein AT3G55790 and two FAD-binding Berberine family proteins (AT1G26380 and AT1G26410) were found to be

highly induced, as well as sulfur E2 (SufE2), a protein likely to play a role in Fe-S cluster assembly (Narayana et al., 2007). Group RII contains genes such as NAS4 and the vacuolar nicotianamine importer ZIF1, both of them induced by Cd, indicating that the plant is activating a heavy metal sequestration program (Mendoza-Cozatl et al., 2011). AOXA1, which is a component of the alternative oxidase branch of mitochondrial respiration, was also found in group RII. AOX expression is correlated with oxidative stress and H<sub>2</sub>O<sub>2</sub> levels, and is expected to be involved in retrograde stress signaling from the mitochondria to the nucleus (Saha et al., 2016). Group RIII contains several genes of interest for Fe homeostasis, most notably the transcription factor genes PYE and MYB72, which are differentially regulated by Cd in the roots of opt3-2 mutants but not of wild-type plants. In opt3-2 roots, these genes are constitutively highly expressed in the absence of Cd but are repressed to wild-type levels in the presence of Cd (Fig. 2D). Other Fe-related allocation genes such as IREG3, HMA3, and FRD3 are also included in this RIII group. Finally, RIV contains the Fe regulon including bHLH38, bHLH39, bHLH100, bHLH101, IRT1, and F6'H1, as well as the transporter genes ZIP3, ZIP9, and MTP3. These genes are all induced by Cd exposure, strongly induced in opt3-2 prior to Cd exposure but repressed after Cd exposure. These and additional transcriptional responses of key genes were further validated by qRT-PCR (Supplementatry Fig. S2). Altogether, these results suggest that Cd triggers an Fe deficiency-like response in wild-type plants, at mild concentrations; however, when combined with other stresses such as Fe excess, different or even opposite transcriptional programs are activated. Notably, this hierarchical regulation of Fe homeostasis seems to apply only to a very specific set of genes and, by imposing different levels of stress, Cd and Cd+Fe excess (opt3-2), we were able to separate clusters with distinct transcriptional patterns.

# Iron deficiency responses are hierarchically regulated based on multiple inputs

In the presence of Fe excess, Cd elicits different responses of Fe deficiency markers in leaves and roots (Fig. 2C, D). While the Cd induction of the subgroup Ib bHLH genes even in the presence of high levels of Fe (opt3-2 leaves) indicates that Cd interferes with Fe sensing, the repression of the FIT network by Cd in opt3-2 roots indicates that the Fe deficiency signals can be over -ridden by other mechanisms (see group RIV in Fig. 2D). In order to better separate the behaviour of these Cd-induced Fe deficiency-responsive genes, we clustered the ferrome genes according to their regulation in response to Cd for each genotype (i.e. Col or opt3-2). Genes which are similarly induced in each genotype were classified as Fe excess independent (Fig. 3, orange dots), as they were induced by Cd despite the high Fe levels in opt3-2 (groups I and II), while those whose regulatory pattern did change (groups III and IV) were classified as Fe excess dependent (Fig. 3, purple dots). Both leaves and

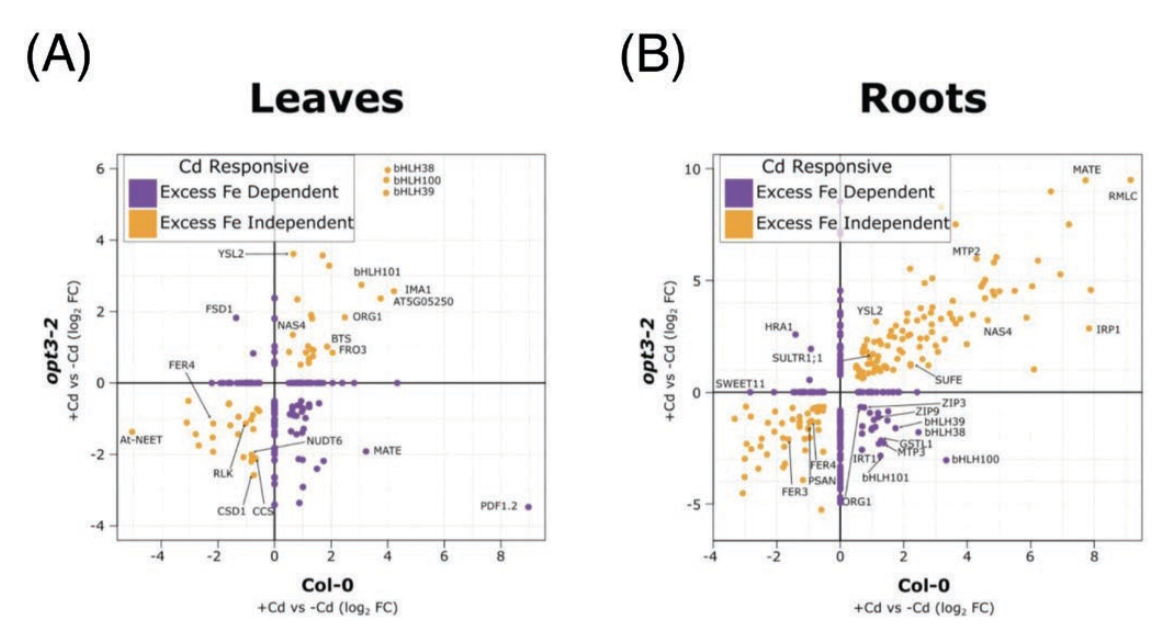


**Fig. 3.** Cadmium-responsive genes are differentially regulated in a tissue-specific manner depending on the Fe levels in plant tissues. (A) Leaf and (B) root Fe deficiency markers similarly induced/repressed by Cd in the wild type and *opt3-2* are labeled as 'Fe excess independent' and shown as orange dots. Fe deficiency markers with opposite expression patterns in the wild type and *opt3-2* during Cd exposure are labeled as 'Fe excess dependent' and shown as purple dots.

roots displayed a combination of Fe excess-dependent and Fe excess-independent gene expression (Fig. 3A, B). Interestingly, some genes whose transcriptional response to Cd was found to be independent of Fe excess in one tissue were found to be dependent on Fe excess in the other. Notably, genes of the subgroup Ib bHLHs were found to be Cd inducible and Fe excess independent in leaves, whereas the same group displayed a different expression pattern in roots: they were induced by Cd in wild-type root systems but repressed in *opt3-2* (i.e. in *opt3-2+Cd*; Fig. 3B).

To further uncover a possible signaling mechanism responsible for separating the Cd-inducible Fe excess-dependent cluster from the Fe excess-independent cluster, we used Gene Ontology (GO) enrichment. This approach allows the identification of broad trends associated with the role of each gene within clusters (Fig. 4). The result from this analysis showed that, in leaves, the Cd-inducible Fe excess-independent cluster was enriched in terms related to Fe or metal ion homeostasis (Fig. 4A), while the Cd-inducible Fe excess-dependent cluster was significantly enriched in terms related to biotic stress (Fig. 4B). Genes related to biotic stress have frequently been observed in mRNA profiling experiments studying Cd stress—an abiotic stress—but the rationale behind this trend is still lacking. Our results, however, suggest that the mechanisms separating the Fe excess-dependent and -independent clusters are closely related to biotic stress responses, which often rely on reactive oxygen species (ROS) for signaling and defense during pathogen infection. In roots, the Fe excess-independent cluster was enriched in terms related to secondary metabolism (Fig. 4C), while the Fe excess-dependent cluster in roots was enriched with

terms relating to nutrient and heavy metal homeostasis (Fig. 4D). This trend also suggests that the mechanism repressing Fe-responsive genes in leaves and roots under Cd exposure is different. In leaves, this may be the result of Cd interfering with Fe sensing, while in roots, a secondary signaling mechanism, probably related to ROS, appears to exert additional transcriptional control on the Fe transcriptional network.

Iron excess and cadmium have additive effects on  $H_2O_2$  accumulation

Our RNA sequencing data consistently show that Cd elicits an Fe deficiency-like response by up-regulating a specific set of transcripts, even in the presence of Fe excess, but also that a significant number of genes originally induced by Cd were repressed to wild-type levels when Fe was in excess (i.e. in opt3-2). These repressed transcripts are disproportionately associated with biotic stress responses and probably share a regulatory component. ROS, such as H<sub>2</sub>O<sub>2</sub>, are generated by the Respiratory Burst Oxidase NADPH protein D (RBOHD) during pathogen attack to mediate defense responses (Miller et al., 2009; Pogány et al., 2009; Maruta et al., 2011; Torres et al., 2013). In leaves, *RBOHD* was induced by Cd in the wild type and induced in opt3-2 without Cd exposure, to levels similar to the wild type exposed to Cd (Supplementarty Fig. S3). Hence, we hypothesized that the repression of some Fe deficiency markers in opt3-2 after Cd exposure may be the result of a H<sub>2</sub>O<sub>2</sub>-mediated transcriptional reprogramming.

To support this hypothesis,  $H_2O_2$  levels were measured in leaves and roots of wild-type and *opt3-2* plants exposed or not

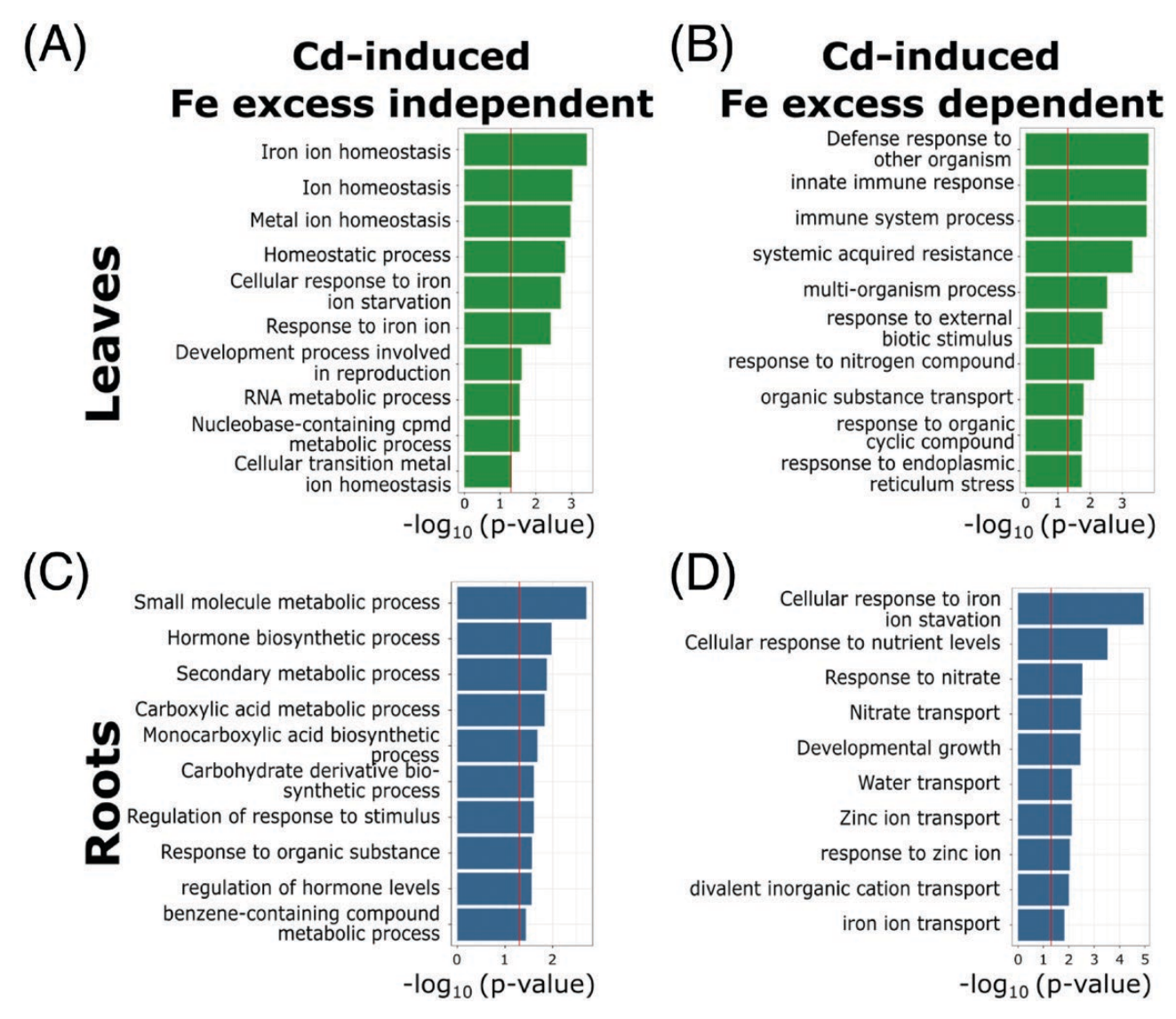


**Fig. 4.** Classification of cadmium-induced genes based on their biological process and sensitivity to Fe excess. Gene Ontology enrichment tests were performed for (A, C) Cd-induced Fe excess-independent and (B, D) -dependent clusters in leaves and roots. The red line indicates the significance threshold (*P*=0.05).

to Cd (Fig. 5). In leaves, exposure to 20 μM Cd had no impact on H<sub>2</sub>O<sub>2</sub> levels, which is consistent with our initial observations that at the times tested, 20 μM Cd has no major impact on leaf metabolism (Fig. 1). opt3-2 plants, however, had significantly more H<sub>2</sub>O<sub>2</sub> compared with wild-type plants, and this difference was more pronounced in the presence of Cd (Fig. 5B). The higher levels of ROS in opt3-2 exposed to Cd, together with the enrichment of ROS-associated genes found through the GO enrichment analysis (Fig. 4A, B), provides a mechanism to explain why some Fe-responsive genes initially induced by Cd in wild-type plants were later repressed by Cd in opt3-2 (i.e. the Cd-inducible Fe excess-dependent cluster, Fig. 3A). Furthermore, it also suggests that when plants simultaneously experience Fe deficiency-like conditions and high ROS, there is a hierarchical regulation of Fe deficiency responses where

ROS prevent the induction of genes that otherwise would have been induced as part of the Fe deficiency response in leaves. Perhaps more interesting is the fact that in leaves, and only in leaves, bHLHs of the subgroup Ib are insensitive to this ROS-mediated hierarchical regulation (Fig. 3A). The  $H_2O_2$  levels in roots followed the same trend as in leaves, but the magnitude of changes was more dramatic. For instance, Cd exposure elevated the  $H_2O_2$  concentration in wild-type roots to levels similar to those found in unexposed *opt3-2*. In addition, Cd increased the  $H_2O_2$  levels in both genotypes, but the concentration of  $H_2O_2$  in *opt3-2* was significantly higher than in the wild type. This higher  $H_2O_2$  content in *opt3-2*, induced by Cd, provides the basis to explain some of the distinct transcriptome profiles observed in roots, where Cd-exposed wild type and unexposed *opt3-2* show similar expression patterns (Fig. 2D, cluster RII),

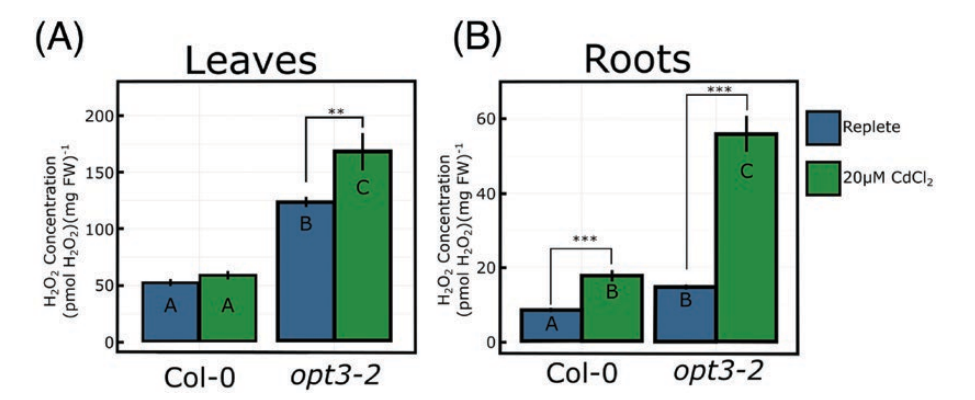


Fig. 5. H<sub>2</sub>O<sub>2</sub> quantification of leaves and roots in wild-type and opt3-2 plants exposed or not to 20 μM CdCl<sub>2</sub> for 72 h (\*\*\*P<0.001, n=6-10).

but the high levels of  $H_2O_2$  in Cd-exposed *opt3-2* repress the expression of the Fe regulon.

# Transient reduction of H<sub>2</sub>O<sub>2</sub> levels in opt3-2 by ROS scavengers

To further test whether ROS, and more specifically H<sub>2</sub>O<sub>2</sub>, are behind the gene repression of Fe/Cd-responsive genes in opt3-2, we aimed to reduce the  $H_2O_2$  levels with ROS scavengers while tracking gene expression. Figure 6A shows that opt3-2 plants fumigated with 10 mM ascorbic acid had negligible levels of H<sub>2</sub>O<sub>2</sub>, measured with the H<sub>2</sub>O<sub>2</sub> oxidation-activated dye PO1. However, in opt3-2 plants exposed to Cd, high H<sub>2</sub>O<sub>2</sub> levels were detected again 2 h after the ascorbic acid treatment and remained higher compared with opt3-2 plants not exposed to Cd. Next, we tested the activity of the promoter region of *OPT3* fused to the firefly luciferase reporter gene in the opt3-2 background. The activity of the OPT3 promoter has been shown to be induced by either Cd exposure or Fe deficiency (Mendoza-Cózatl et al., 2014; Khan et al., 2018); however, the activity of this reporter is repressed in opt3-2 exposed to Cd compared with non-treated plants (Fig. 6B). Thus, the opt3-2×OPT3p::Luc line offers a unique system to test the expression of a Fe/ Cd-responsive marker repressed when H<sub>2</sub>O<sub>2</sub> levels are high. Figure 6B shows that fumigation with 10 mM ascorbate restores the activity of OPT3p::Luc in opt3-2 plants treated with Cd to levels similar to untreated plants. Similar results were achieved by infiltrating plants with reducing agents such as glutathione and DTT (Supplementary Fig. S4), demonstrating that the use of H<sub>2</sub>O<sub>2</sub> scavengers can restore the expression of Fe/Cd-responsive genes originally repressed by high levels of H<sub>2</sub>O<sub>2</sub> in the opt3-2 background.

Impaired photosynthetic efficiency and Fe–S metabolism as sources for elevated  $H_2O_2$  levels in opt3-2

Cd is unable to produce ROS through the Fenton reaction (Strlič et al., 2003); however, Cd does generate ROS through

displacement of Fe from the active site of proteins and other molecules, and photosynthesis is known to be particularly sensitive to Cd toxicity (Küpper *et al.*, 2007; Parmar *et al.*, 2013). To determine if the increased  $H_2O_2$  levels in Cd-exposed *opt3-2* leaves could be explained in part by an impaired photosynthetic apparatus, the maximum potential quantum efficiency of PSII ( $F_v/F_m$ ) was measured in wild-type and *opt3-2* plants using an Imaging-PAM system (Fig. 7A). The results show that photosynthesis in *opt3-2* remained unaffected under control conditions; however, a 20% reduction in  $F_v/F_m$ , predominantly originating from younger leaves, was found after Cd exposure (Fig. 7B, C).

Fe-S metabolism has also been implicated in Fe and ROS homeostasis and, more recently, AtNEET, an Fe-S donor protein in the chloroplast, has been identified as a key protein regulating Fe-S homeostasis and ROS production. More specifically, the inability of AtNEET to transfer Fe-S clusters triggers an Fe deficiency-like transcript profile (Zandalinas et al., 2019). To determine if Cd impairs the stability and/or the ability of AtNEET to transfer 2Fe-2S clusters, we performed AtNEET stability and 2Fe-2S transfer experiments at different Cd concentrations using UV-Vis spectroscopy (Fig. 8). The loss of the characteristic absorption peak of the holo-AtNEET at 458 nm shows that AtNEET is a labile protein prone to dissociation in the presence of Cd (Fig. 8A). Next, we asked if Cd could also impair the 2Fe-2S transfer from AtNEET to the acceptor protein ferredoxin (Fd). In the absence of Cd, the transfer of 2Fe-2S clusters between AtNEET and Fd can be tracked by following the 458-428 nm spectral shift indicating the 2Fe-2S transfer from the holo-AtNEET to the holo-Fd peak (Fig. 8B, inset; Zandalinas et al., 2019). Notably, the efficiency of this transfer was impaired by Cd (Fig. 8B), and quantification of the absorbances at each characteristic peak showed significant decreases in the Fe-S transfer efficiency at Cd concentrations as low as 5 µM Cd (Fig. 8C). These results were further confirmed by PAGE analyses where a clear loss of the holo-Fd formation was observed as early as 10 min after Cd exposure (Supplementary Fig. S5A, B). Taken together, these data suggest that the elevated H<sub>2</sub>O<sub>2</sub> levels induced by Cd are the result of an additive impairment of photosynthesis

(A)

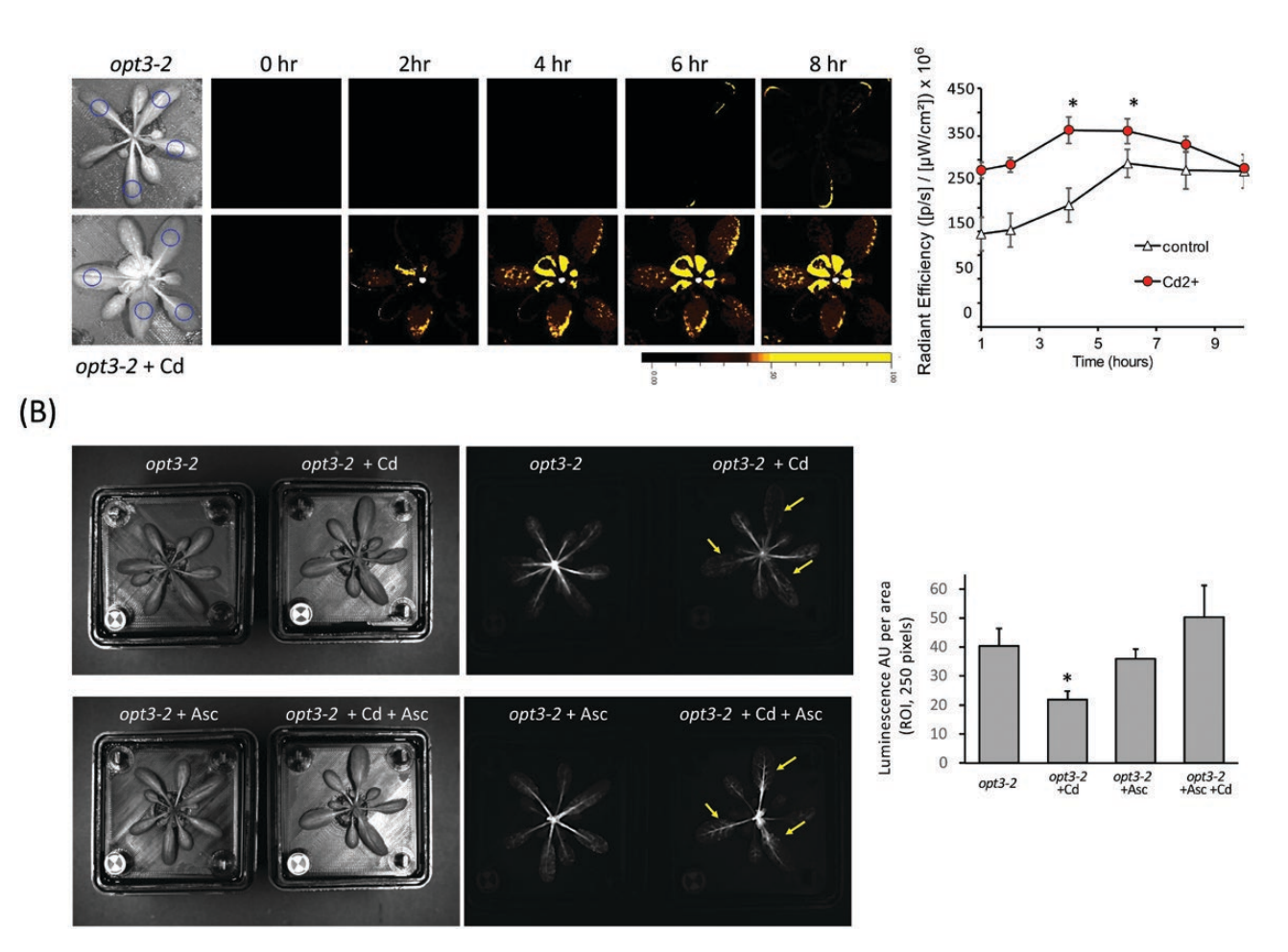


Fig. 6. Dynamic imaging of  $H_2O_2$  in opt3-2 plants exposed to cadmium in the presence of  $H_2O_2$  scavengers. (A) opt3-2 plants exposed or not to cadmium were fumigated first with 10 mM ascorbic acid for 30 min followed by a second fumigation with the  $H_2O_2$  oxidation-activated dye Peroxy Orang 1 for an additional 30 min. Plants were continuously imaged on an IVIS Lumina S5 fluorescence detector (excitation/emission 540 nm/620 nm). Asterisks denote statistical differences (P<0.05; t-test) compared with t=0. Experiments were repeated three times with similar results. (B)  $opt3-2 \times OPT3$ ::Luc plants exposed or not to Cd were first sprayed with 5 mM luciferin, imaged in a luminescence detector (15 min exposure time,  $4 \times 4$  binning settings) followed by fumigation with 10 mM ascorbic acid. Luminescence was quantified on four regions of interest (ROI) for a second time with identical settings using ImageJ/FIJI. The ROI represents a circular area corresponding to 250 pixels beginning at the base of the petiole of mature leaves. Experiments were repeated three times with similar results. Asterisks denote statistical differences (P<0.05; t-test) compared with plants not exposed to Cd.

and Fe–S homoeostasis. In turn, the different  $H_2O_2$  levels induced by Cd in the wild type and *opt3-2* provide a mechanism to explain the particular clustering of Cd-induced Fe excess-dependent and -independent genes observed between wild-type and *opt3-2* genotypes.

# **Discussion**

Cadmium has long been known to induce genes that are up-regulated when plants experience Fe deficiency and, traditionally, this has been attributed to a reduced Fe influx into the plant as Cd competes with Fe for the same uptake mechanism in roots (i.e. IRT1). Here we provide evidence suggesting that

Cd also interferes with Fe sensing, thus leading to transcriptional programs consistent with an Fe deficiency response. Our data also suggest that Fe deficiency responses are regulated by different inputs in a tissue-specific manner and that some Fe deficiency signals, particularly in roots, can be partially over-ridden by oxidative stress. Such hierarchical regulation of Fe homeostasis would prevent further oxidative damage when plants experience opposite cues such as Fe deficiency in the presence of high levels of H<sub>2</sub>O<sub>2</sub>

Iron deficiency responses are regulated by several and independent inputs

To test the extent of Fe deficiency response induced by Cd, we first compiled different datasets and assembled root- and

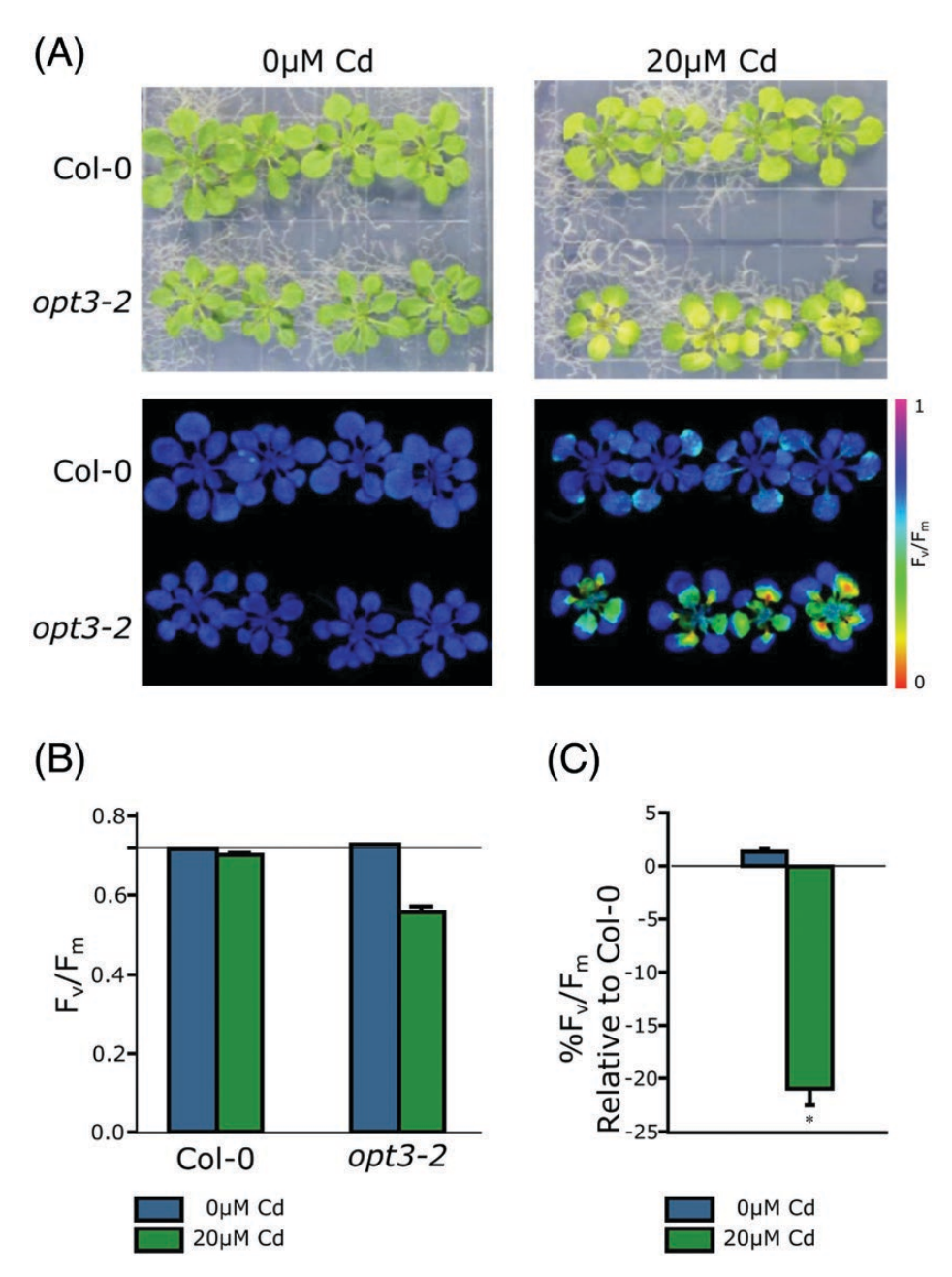


**Fig. 7.** Photosynthesis in opt3-2 plants is particularly sensitive to cadmium. Photosynthetic efficiency of Col-0 (wild type) and opt3-2 was measured in the presence or absence of 20  $\mu$ M CdCl<sub>2</sub>. (A) RGB (top) and  $F_{\nu}/F_{\rm m}$  false color images (bottom) show increased chlorosis and photosynthetic inhibition in opt3-2. (B) Photosynthetic efficiency and (C) reduction in photosynthetic efficiency in wild-type and opt3-2 plants exposed or not to 20  $\mu$ M CdCl<sub>2</sub>. Error bars indicate the SE of eight individual plants meaured in each experiment.

shoot-specific lists of genes consistently deregulated in response to Fe deficiency (expanded root ferrome and the leaf ferrome, Supplementary Table S1). After comparing these tissue-specific ferrome datasets with our Cd-induced transcriptome in wild-type plants, we found a large overlap of genes deregulated by Cd, ~60% of the Fe deficiency markers, including members of the FIT network, PYE network, and a recently described family of peptides that regulate Fe deficiency responses known as IMAs (Fig. 2; Supplementary Tables S2–S4). If these

responses were only the result of uptake competition between Cd and Fe at the root level, this Cd-induced transcriptional response should not occur in plants that accumulate high levels of Fe within their tissues (i.e. *opt3* mutants). However, for some of these genes, Cd still induced a strong Fe deficiency response regardless of the high levels of Fe present in plant tissues (Fig. 2C, LI). In other cases, the presence of high Fe levels influenced the magnitude of the transcriptional response to Cd or caused opposite effect on gene expression compared with wild-type

# Page 12 of 15 | McInturf et al.

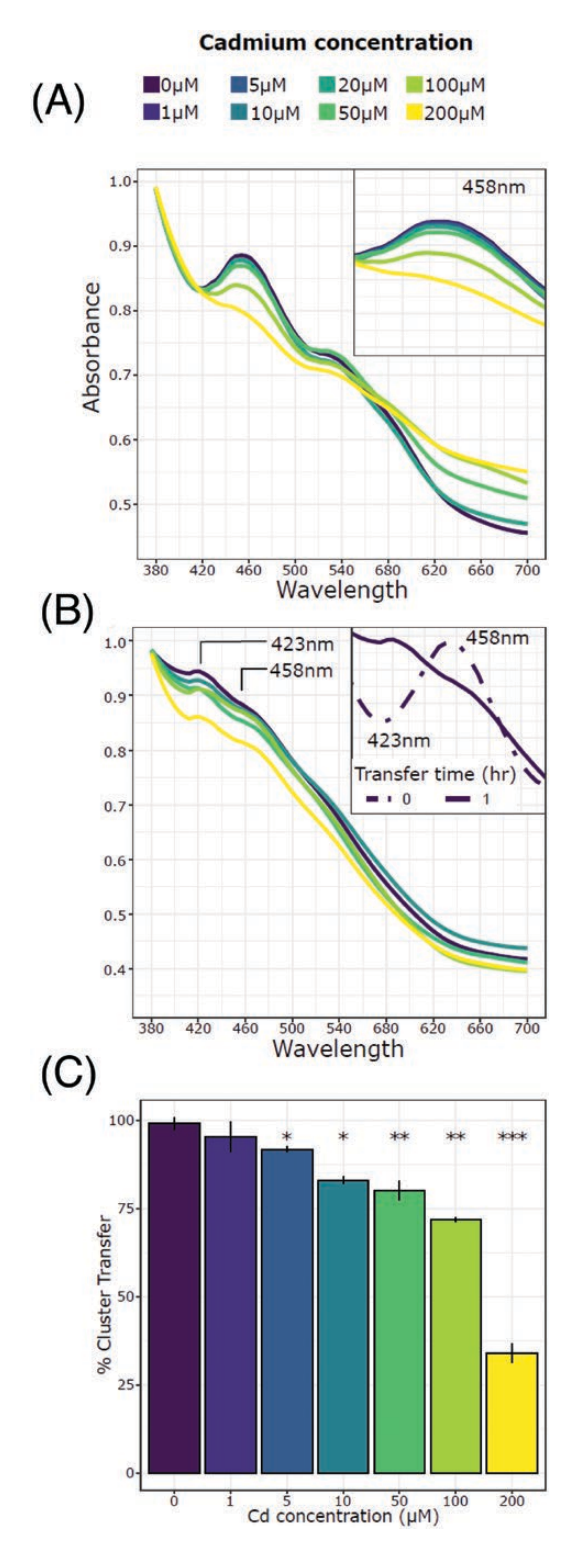


**Fig. 8.** Exposure to Cd impairs AtNEET stability and its capacity to transfer 2Fe–2S clusters to ferrodoxin. (A) Absorbance spectra of recombinant AtNEET protein 6 h following the addition of Cd; the separation of the peak characteristic absorption at 458 nm reflects the loss of the Fe–S cluster from AtNEET. (B) In the presence of ferredoxin (characteristic peak 423 nm), AtNEET is able to transfer its 2Fe–2S in 1 h (inset) which is impaired by increased Cd concentrations. (C) Percentage of 2Fe–2S clusters transferred from AtNEET to ferredoxin from (B), \*P<0.01, \*\*P<0.001, \*\*P<0.0001.

plants (Fig. 3, purple dots). This complex and diverse pattern of gene expression indicated that the effects of Cd on genes associated with Fe deficiency were due to more than the direct effect of Cd on Fe uptake. Further clustering analyses allowed us to separate and define specific gene clusters, and we found that some of these clusters are associated with biotic stress and ROS levels. Notably, specific clusters of genes known to be expressed in specific tissues (i.e. the vasculature) were induced by Cd regardless of the Fe and ROS levels in plant tissues. This additional information suggested that Fe sensing and Fe deficiency responses are organized in discrete clusters and that the magnitude and direction of transcriptional responses are cluster specific based on the actual levels of Fe, ROS, and, in this case, the presence of Cd.

# Cadmium impairs iron sensing

The precise location of Fe sensing in plants is still unclear, but recent data, including this work, suggest that Fe levels may be sensed independently throughout the plant in a tissue- and cellspecific manner (Fig. 2; Khan et al., 2018). For instance, leaves of opt3 mutants (opt3-2 and opt3-3) overaccumulate Fe and consequently opt3 leaves show a transcriptional program consistent with an Fe overload (Khan et al., 2018); however, the phloem sap of opt3 mutants has half of the Fe levels compared with wild-type plants (Zhai et al., 2014). Yet, Fe deficiency markers known to be located in the leaf vasculature such as bHLH38/39/100/101 are not induced in opt3-2 leaves (Fig. 2C, LI). These results suggest that the high levels of Fe in the leaf apoplast, outside companion cells, may be sufficient to prevent the induction of Fe deficiency genes in companion cells, even if the Fe levels inside companion cells are low (Zhai et al., 2014). Alternatively, Fe excess and Fe deficiency may be sensed by independent pathways and, when companion cells receive conflicting information (i.e. low levels of Fe in the cytosol but high Fe levels in the apoplast), the Fe excess signaling prevails. Interestingly, our study also found that the bHLH38/39/100/101 cluster is highly induced by Cd in opt3-2 leaves (Fig. 2C, LI), and this induction is insensitive to the high levels of H<sub>2</sub>O<sub>2</sub> detected in opt3-2 leaves (Fig. 5A). Moreover, this induction requires only a trace amount of Cd as opt3 leaves accumulate minimal levels of Cd compared with the wild type (Mendoza-Cózatl et al., 2014). Altogether, these results suggest that in leaves, and more specifically in companion cells, Cd impairs Fe sensing and that this vascular-specific signaling pathway is insensitive to negative regulators such as Fe excess.

Iron deficiency is hierarchically regulated by competing nutrient acquisition and oxidative stress signals

Additional evidence for independent tissue-specific Fe-sensing mechanisms came from the finding that the transcription of some genes is oppositely regulated in leaves and roots. For instance, while bHLH38/39/100/101 are Cd induced and Fe excess independent in leaves, they are Cd induced but Fe excess dependent in roots (Fig. 2D). Notably,

this severe repression in roots extends to other well-known Fe deficiency markers such as ORG1 (Kang et al., 2003) and FRO3 (Jain et al., 2014), suggesting that transcriptional repression by Cd in opt3-2 roots is under the control of additional inputs. This apparent inconsistency prompted us to explore the nature of these additional inputs. High H<sub>2</sub>O<sub>2</sub> levels have been previously shown to inhibit Fe deficiency responses (Le et al., 2016), and our H<sub>2</sub>O<sub>2</sub> measurements show that there were significant differences across genotypes, tissues, and treatments (Fig. 5A, B). In particular, opt3 roots exposed to Cd contained three times more H<sub>2</sub>O<sub>2</sub> than the wild type. This dramatic increase in H<sub>2</sub>O<sub>2</sub> levels induced by Cd provides a mechanistic explanation for the repression of Fe deficiency markers in opt3-2 roots, probably mediated by ZAT12 or proteins with similar function (Le et al., 2016). As for the source of these high Cd-induced ROS levels, it has been shown that Cd uncouples the mitochondrial electron transport chain, and Fe displacement or inhibition of Fe-containing enzymes by Cd could be another source of H<sub>2</sub>O<sub>2</sub> in roots (for a review, see Valerio Branca et al., 2020).

In leaves, Cd also induced significantly higher H<sub>2</sub>O<sub>2</sub> levels in opt3-2 than in wild-type plants, and yet some Fe-responsive genes were highly induced despite the high Fe and H<sub>2</sub>O<sub>2</sub> levels (Fig. 2C, LI cluster) while others were repressed, including the promoter activity of OPT3 measured by activity of the firefly luciferase reporter gene. Interestingly, this repression can be reverted in opt3-2 plants exposed to Cd by H<sub>2</sub>O<sub>2</sub> scavengers such as ascorbic acid, glutathione, and DTT (Fig. 6B; Supplementary Fig. S4). Chloroplast metabolism and photosynthesis are highly dependent on redox reactions and therefore are highly sensitive to Cd (Parmar et al., 2013). In turn, our photosynthetic efficiency measurements confirmed that Cd has a higher inhibitory effect in opt3-2 leaves compared with wild-type plants (Fig. 7) and suggest that in opt3-2 leaves, chloroplasts are a significant source of H<sub>2</sub>O<sub>2</sub>. In fact, this increase in ROS was similar to what was observed in the dominant-negative H89C AtNEET mutant, which exhibits both higher H<sub>2</sub>O<sub>2</sub> levels and impaired Fe homeostasis due to the impaired transfer of 2Fe–2S clusters from AtNEET to acceptor proteins (Zandalinas et al., 2019). This same inhibitory 2Fe-2S transfer effect was found in vitro in the presence of low levels of Cd (Fig 8B, C). Hence, a Cd-dependent impairment of Fe-S homeostasis, combined with inhibition of PSII, provides a mechanistic basis for the elevated levels of H<sub>2</sub>O<sub>2</sub> and the consequent partitioning of Cd-induced Fe excess-dependent and -independent gene clusters. In summary, our results suggest that when plants experience opposite cues (i.e. Fe deficiency and high ROS levels), there is a hierarchical regulation of Fe homeostasis in which ROS over-ride the induction of specific transcriptional programs that otherwise would have been induced by Fe deficiency.

# Supplementary data

The following supplementary data are available at *JXB* online.

Fig. S1. Venn diagrams showing gene expression relationships during Cd exposure.

Fig. S2. Validation of gene RNA-seq data by qRT-PCR.

Fig. S3. eFP browser expression data for RBOHD/F.

Fig. S4. Expression of Cd/Fe-inducible markers in *opt3-2*.

Fig. S5. Native PAGE separation of AtNEET and ferredoxin.

Table S1. Expanded root ferrome and leaf ferrome.

Table S2. Counts per million and log2 fold changes between genotypes and treatments.

Table S3. Iron marker genes used to generate the Venn diagrams shown in Fig. 2.

Table S4. Cd-responsive Fe excess-dependent and -independent genes.

Table S5. Primers used for qRT-PCR validation of RNA-seq results.

#### **Author contributions**

SAM, MAK, NACG, AG, JL, RH, H-HK, H-BM, YF: conducting the experiments; SAM, DMC, MAK, FLG, H-HK, MK, and RM writing the manuscript.

# **Funding**

This work was supported by funding from the National Science Foundation (IOS-1734145 and MCB-1818312 to DMC, NSF-BSF MCB-1936590 and IOS-1932639 to RM, OIA-1430427 to FLG, and BSF 2015831 to RN), National Research Foundation, South Africa (NRF-116346 and NRF-109083 to MK), the Bond Life Sciences Early Concept Grant (DGMC and RM), and the University of Missouri. H-HK received funding from a National Science Foundation Career Award (IOS-1553506) and a third call ERA-CAPS grant from the National Science Foundation (IOS-1847382). Collaborative research between the DMC and MK groups is funded by a DST-NRF Centre of Excellence in Food Security award (Project ID 170202).

# Data availability

RNA-seq data (without Cd treatment) can be found on NCBI GEO GSE79275, while Cd-exposed data are available as GSE128156. These datasets comprise the SuperSeries GSE128157.

# References

Ahmad S, Van Hulten M, Martin J, Pieterse CM, Van Wees SC, Ton J. 2011. Genetic dissection of basal defence responsiveness in accessions of *Arabidopsis thaliana*. Plant, Cell & Environment **34**, 1191–1206.

Barberon M, Zelazny E, Robert S, Conéjéro G, Curie C, Friml J, Vert G. 2011. Monoubiquitin-dependent endocytosis of the iron-regulated transporter 1 (IRT1) transporter controls iron uptake in plants. Proceedings of the National Academy of Sciences, USA 108, E450–E458.

**Barrett T, Wilhite SE, Ledoux P, et al.** 2013. NCBI GEO: archive for functional genomics data sets—update. Nucleic Acids Research **41**, D991–D995.

**Benjamini Y, Hochberg Y.** 1995. Controlling the false discovery rate: a practical and powerful approach to multiple testing. Journal of the Royal Statistical Society. Series B (Methodological) **57**, 289–300.

# Page 14 of 15 | McInturf et al.

- **Brumbarova T, Le C, Bauer P.** 2016. Hydrogen peroxide measurement in arabidopsis root tissue using Amplex red. Bio-protocol **6**, doi: 10.21769/Bio-Protocol Bio-Protocol Bio-Pro
- **Buckhout TJ, Yang TJ, Schmidt W.** 2009. Early iron-deficiency-induced transcriptional changes in Arabidopsis roots as revealed by microarray analyses. BMC Genomics **10**. 147.
- **Cabot C, Gallego B, Martos S, Barceló J, Poschenrieder C.** 2013. Signal cross talk in Arabidopsis exposed to cadmium, silicon, and *Botrytis cinerea*. Planta **237**, 337–349.
- **Connolly EL, Fett JP, Guerinot ML.** 2002. Expression of the IRT1 metal transporter is controlled by metals at the levels of transcript and protein accumulation. The Plant Cell **14**, 1347–1357.
- Curie C, Cassin G, Couch D, Divol F, Higuchi K, Le Jean M, Misson J, Schikora A, Czernic P, Mari S. 2009. Metal movement within the plant: contribution of nicotianamine and yellow stripe 1-like transporters. Annals of Botany 103, 1–11.
- **Curie C, Panaviene Z, Loulergue C, Dellaporta SL, Briat JF, Walker EL.** 2001. Maize *yellow stripe1* encodes a membrane protein directly involved in Fe(III) uptake. Nature **409**, 346–349.
- Falcon S, Gentleman R. 2007. Using GOstats to test gene lists for GO term association. Bioinformatics 23, 257–258.
- **Fichman Y, Miller G, Mittler R.** 2019. Whole-plant live imaging of reactive oxygen species. Molecular Plant **12**, 1203–1210.
- **García MJ, Lucena C, Romera FJ, Alcántara E, Pérez-Vicente R.** 2010. Ethylene and nitric oxide involvement in the up-regulation of key genes related to iron acquisition and homeostasis in Arabidopsis. Journal of Experimental Botany **61**, 3885–3899.
- **Grillet L, Lan P, Li W, Mokkapati G, Schmidt W.** 2018. IRON MAN, a ubiquitous family of peptides that control iron transport in plants. Nature Plants **4**, 953–963.
- **Guillaume D, Neveu J, Zelazny E, Vert G.** 2018. Metal sensing by the IRT1 transporter-receptor orchestrates its own degradation and plant metal nutrition. Molecular Cell **69**, 953–964.
- **Hindt MN, Akmakjian GZ, Pivarski KL, Punshon T, Baxter I, Salt DE, Guerinot ML.** 2017. BRUTUS and its paralogs, BTS LIKE1 and BTS LIKE2, encode important negative regulators of the iron deficiency response in *Arabidopsis thaliana*. Metallomics **9**, 876–890.
- **Hindt MN, Guerinot ML.** 2012. Getting a sense for signals: regulation of the plant iron deficiency response. Biochimica et Biophysica Acta **1823**, 1521–1530.
- **Hirayama T, Lei GJ, Yamaji N, Nakagawa N, Ma JF.** 2018. The putative peptide gene FEP1 regulates iron deficiency response in Arabidopsis. Plant & Cell Physiology **59**, 1739–1752.
- **Huber W, Carey VJ, Gentleman R, et al.** 2015. Orchestrating high-throughput genomic analysis with Bioconductor. Nature Methods **12**, 115–121.
- Inoue H, Kobayashi T, Nozoye T, Takahashi M, Kakei Y, Suzuki K, Nakazono M, Nakanishi H, Mori S, Nishizawa NK. 2009. Rice OsYSL15 is an iron-regulated iron (III)-deoxymugineic acid transporter expressed in the roots and is essential for iron uptake in early growth of the seedlings. Journal of Biological Chemistry **284**, 3470–3479.
- **Jain A, Wilson GT, Connolly EL.** 2014. The diverse roles of FRO family metalloreductases in iron and copper homeostasis. Frontiers in Plant Science **5**, 1–6.
- **Kang HG, Foley RC, Oñate-Sánchez L, Lin C, Singh KB.** 2003. Target genes for OBP3, a Dof transcription factor, include novel basic helix-loophelix domain proteins inducible by salicylic acid. The Plant Journal **35**, 362–372.
- **Khan MA, Castro-Guerrero NA, McInturf SA, et al.** 2018. Changes in iron availability in Arabidopsis are rapidly sensed in the leaf vasculature and impaired sensing leads to opposite transcriptional programs in leaves and roots. Plant, Cell & Environment **41**, 2263–2276.
- **Khan MA, Castro-Guerrero N, Mendoza-Cozatl DG.** 2014. Moving toward a precise nutrition: preferential loading of seeds with essential nutrients over non-essential toxic elements. Frontiers in Plant Science **5**, 51.

- Kim D, Pertea G, Trapnell C, Pimentel H, Kelley R, Salzberg SL. 2013. TopHat2: accurate alignment of transcriptomes in the presence of insertions, deletions and gene fusions. Genome Biology 14, R36.
- Korshunova YO, Eide D, Clark WG, Guerinot ML, Pakrasi HB. 1999. The IRT1 protein from *Arabidopsis thaliana* is a metal transporter with a broad substrate range. Plant Molecular Biology **40**, 37–44.
- Kumar RK, Chu H-H, Abundis C, Vasques K, Chan-Rodriguez D, Chia J-C, Huang R, Vatamaniuk OK, Walker EL. 2017. Ironnicotianamine transporters are required for proper long distance iron signaling. Plant Physiology **175**, 1254–1268.
- Kunz HH, Scharnewski M, Feussner K, Feussner I, Flügge UI, Fulda M, Gierth M. 2009. The ABC transporter PXA1 and peroxisomal beta-oxidation are vital for metabolism in mature leaves of Arabidopsis during extended darkness. The Plant Cell **21**, 2733–2749.
- **Küpper H, Parameswaran A, Leitenmaier B, Trtílek M, Šetlík I.** 2007. Cadmium-induced inhibition of photosynthesis and long-term acclimation to cadmium stress in the hyperaccumulator *Thlaspi caerulescens*. New Phytologist **175**, 655–674.
- Le CT, Brumbarova T, Ivanov R, Stoof C, Weber E, Mohrbacher J, Fink-Straube C, Bauer P. 2016. ZINC FINGER OF ARABIDOPSIS THALIANA12 (ZAT12) interacts with FER-LIKE IRON DEFICIENCY-INDUCED TRANSCRIPTION FACTOR (FIT) linking iron deficiency and oxidative stress responses. Plant Physiology 170, 540–557.
- Lee S, Chiecko JC, Kim SA, Walker EL, Lee Y, Guerinot ML, An G. 2009. Disruption of OsYSL15 leads to iron inefficiency in rice plants. Plant Physiology **150**, 786–800.
- **Lešková A, Giehl RFH, Hartmann A, Fargašová A, von Wirén N.** 2017. Heavy metals induce iron deficiency responses at different hierarchic and regulatory levels. Plant Physiology **174**, 1648–1668.
- **Li X, Zhang H, Ai Q, Liang G, Yu D.** 2016. Two bHLH transcription factors, bHLH34 and bHLH104, regulate iron homeostasis in *Arabidopsis thaliana*. Plant Physiology **170**, 2478–2493.
- **Liang G, Zhang H, Li X, Ai Q, Yu D.** 2017. bHLH transcription factor bHLH115 regulates iron homeostasis in *Arabidopsis thaliana*. Journal of Experimental Botany **68**, 1743–1755.
- Lingam S, Mohrbacher J, Brumbarova T, Potuschak T, Fink-Straube C, Blondet E, Genschik P, Bauer P. 2011. Interaction between the bHLH transcription factor FIT and ETHYLENE INSENSITIVE3/ETHYLENE INSENSITIVE3-LIKE1 reveals molecular linkage between the regulation of iron acquisition and ethylene signaling in *Arabidopsis*. The Plant Cell **23**, 1815–1829.
- Long TA, Tsukagoshi H, Busch W, Lahner B, Salt DE, Benfey PN. 2010. The bHLH transcription factor POPEYE regulates response to iron deficiency in Arabidopsis roots. The Plant Cell **22**, 2219–2236.
- Maruta T, Inoue T, Tamoi M, Yabuta Y, Yoshimura K, Ishikawa T, Shigeoka S. 2011. Arabidopsis NADPH oxidases, AtrohD and AtrohF, are essential for jasmonic acid-induced expression of genes regulated by MYC2 transcription factor. Plant Science 180, 655–660.
- Meda AR, Scheuermann EB, Prechsl UE, Erenoglu B, Schaaf G, Hayen H, Weber G, von Wirén N. 2007. Iron acquisition by phytosiderophores contributes to cadmium tolerance. Plant Physiology **143**, 1761–1773.
- **Mendoza-Cózatl DG, Jobe TO, Hauser F, Schroeder JI.** 2011. Longdistance transport, vacuolar sequestration, tolerance, and transcriptional responses induced by cadmium and arsenic. Current Opinion in Plant Biology **14**, 554–562.
- **Mendoza-Cózatl DG, Xie Q, Akmakjian GZ, et al.** 2014. OPT3 is a component of the iron-signaling network between leaves and roots and misregulation of OPT3 leads to an over-accumulation of cadmium in seeds. Molecular Plant **7**, 1455–1469.
- Miller G, Schlauch K, Tam R, Cortes D, Torres MA, Shulaev V, Dangl JL, Mittler R. 2009. The plant NADPH oxidase RBOHD mediates rapid systemic signaling in response to diverse stimuli. Science Signaling 2, ra45.
- Morgan M, Anders S, Lawrence M, Aboyoun P, Pagès H, Gentleman R. 2009. ShortRead: a bioconductor package for input, quality assessment and exploration of high-throughput sequence data. Bioinformatics 25, 2607–2608.

- Narayana MUM, Pilon M, Fontecave M, Ye H, Rousset C, Pilon-Smits EAH, Abdel-Ghany SE, Ollagnier-de-Choudens S, Sanakis Y. 2007. Characterization of *Arabidopsis thaliana* SufE2 and SufE3. Journal of Biological Chemistry **282**, 18254–18264.
- **Nechushtai R, Conlan AR, Harir Y, et al.** 2012. Characterization of Arabidopsis NEET reveals an ancient role for NEET proteins in iron metabolism. The Plant Cell **24**, 2139–2154.
- **Parmar P, Kumari N, Sharma V.** 2013. Structural and functional alterations in photosynthetic apparatus of plants under cadmium stress. Botanical Studies **54**, 45.
- Pogány M, von Rad U, Grün S, Dongó A, Pintye A, Simoneau P, Bahnweg G, Kiss L, Barna B, Durner J. 2009. Dual roles of reactive oxygen species and NADPH oxidase RBOHD in an Arabidopsis–Alternaria pathosystem. Plant Physiology **151**, 1459–1475.
- **R Core Team**. 2018. R: a language and environment for statistical computing. Vienna, Austria: R Foundation for Statistical Computing.
- **Robinson MD, McCarthy DJ, Smyth GK.** 2010. edgeR: a Bioconductor package for differential expression analysis of digital gene expression data. Bioinformatics **26**, 139–140.
- Robinson NJ, Procter CM, Connolly EL, Guerinot ML. 1999. A ferric-chelate reductase for iron uptake from soils. Nature **397**, 694–697.
- **Römheld V, Marschner H.** 1986. Mobilization of iron in the rhizosphere of different plant species. Advances in Plant Nutrition **2**, 155–204.
- **Saha B, Borovskii G, Panda SK.** 2016. Alternative oxidase and plant stress tolerance. Plant Signaling & Behavior **11**, e1256530.
- **Santi S, Schmidt W.** 2009. Dissecting iron deficiency-induced proton extrusion in Arabidopsis roots. New Phytologist **183**, 1072–1084.
- **Schmidt W, Buckhout TJ.** 2011. A hitchhiker's guide to the Arabidopsis ferrome. Plant Physiology and Biochemistry **49**, 462–470.
- **Selote D, Samira R, Matthiadis A, Gillikin JW, Long TA.** 2015. Ironbinding E3 ligase mediates iron response in plants by targeting basic helix–loop–helix transcription factors. Plant Physiology **167**, 273–286.
- **Sivitz A, Grinvalds C, Barberon M, Curie C, Vert G.** 2011. Proteasome-mediated turnover of the transcriptional activator FIT is required for plant iron-deficiency responses. The Plant Journal **66**, 1044–1052.
- **Sivitz AB, Hermand V, Curie C, Vert G.** 2012. Arabidopsis bHLH100 and bHLH101 control iron homeostasis via a FIT-independent pathway. PLoS One **7** e44843.
- **Stein RJ, Waters BM.** 2012. Use of natural variation reveals core genes in the transcriptome of iron-deficient *Arabidopsis thaliana* roots. Journal of Experimental Botany **63**, 1039–1055.
- **Strlič M, Kolar J, Šelih VS, Kočar D, Pihlar B.** 2003. A comparative study of several transition metals in Fenton-like reaction systems at circum-neutral pH. Acta Chimica Slovenica **50**, 619–632.
- Torres MA, Morales J, Sánchez-Rodríguez C, Molina A, Dangl JL. 2013. Functional interplay between Arabidopsis NADPH oxidases and heterotrimeric G protein. Molecular Plant-Microbe Interactions 26, 686–694.

- **Urzica EI, Casero D, Yamasaki H, et al.** 2012. Systems and *trans*-system level analysis identifies conserved iron deficiency responses in the plant lineage. The Plant Cell **24**, 3921–3948.
- Valerio Branca JJ, Pacini A, Gulisano M, Taddei N, Fiorillo C, Becatti M, 2020. Cadmium-induced cytotoxicity: effects on mitochondrial electron transport chain. Frontiers in Cell and Developmental Biology 8, 604377.
- **Velikova V, Yordanov I, Edreva A.** 2000. Oxidative stress and some antioxidant systems in acid rain-treated bean plants: protective role of exogenous polyamines. Plant Science **151**, 59–66
- Wang N, Cui Y, Liu Y, Fan H, Du J, Huang Z, Yuan Y, Wu H, Ling HQ. 2013. Requirement and functional redundancy of lb subgroup bHLH proteins for iron deficiency responses and uptake in *Arabidopsis thaliana*. Molecular Plant **6**, 503–513.
- Wang L, Tsuda K, Truman W, Sato M, Nguyen le V, Katagiri F, Glazebrook J. 2011. CBP60g and SARD1 play partially redundant critical roles in salicylic acid signaling. The Plant Journal 67, 1029–1041.
- **Warnes GR, Bolker B, Bonebakker L, et al.** 2016. Gplots: various R programming tools for plotting data. https://cran.r-project.org/web/packages/gplots/index.html
- **Wu H, Chen C, Du J, et al.** 2012. Co-overexpression FIT with AtbHLH38 or AtbHLH39 in Arabidopsis-enhanced cadmium tolerance via increased cadmium sequestration in roots and improved iron homeostasis of shoots. Plant Physiology **158**, 790–800.
- Yang Y, Ou B, Zhang J, Si W, Gu H, Qin G, Qu LJ. 2014. The Arabidopsis Mediator subunit MED16 regulates iron homeostasis by associating with EIN3/EIL1 through subunit MED25. The Plant Journal 77, 838–851.
- Yuan Y, Wu H, Wang N, Li J, Zhao W, Du J, Wang D, Ling HQ. 2008. FIT interacts with AtbHLH38 and AtbHLH39 in regulating iron uptake gene expression for iron homeostasis in Arabidopsis. Cell Research 18, 385–397.
- **Zandalinas SI, Song L, Sengupta S, et al.** 2019. Expression of a dominant-negative AtNEET-H89C protein disrupts iron-sulfur metabolism and iron homeostasis in Arabidopsis. The Plant Journal **101**, 1152–1169.
- **Zarei A, Körbes AP, Younessi P, Montiel G, Champion A, Memelink J.** 2011. Two GCC boxes and AP2/ERF-domain transcription factor ORA59 in jasmonate/ethylene-mediated activation of the PDF1.2 promoter in Arabidopsis. Plant Molecular Biology **75**, 321–331.
- **Zhai Z, Gayomba SR, Jung H, et al.** 2014. OPT3 is a phloem-specific iron transporter that is essential for systemic iron signaling and redistribution of iron and cadmium in Arabidopsis. The Plant Cell **26**, 2249–2264.
- Zhang J, Liu B, Li M, Feng D, Jin H, Wang P, Liu J, Xiong F, Wang J, Wang HB. 2015. The bHLH transcription factor bHLH104 interacts with IAA-LEUCINE RESISTANT3 and modulates iron homeostasis in Arabidopsis. The Plant Cell 27, 787–805.
- **Zhang L, Tan Q, Lee R, Trethewy A, Lee YH, Tegeder M.** 2010. Altered xylem-phloem transfer of amino acids affects metabolism and leads to increased seed yield and oil content in Arabidopsis. The Plant Cell **22**, 3603–3620.